PHYSICS AND CHEMISTRY OF SOLID STATE
V. 26, No.1 (2025) pp. 166-173
Section: Chemistry

DOI: 10.15330/pcss.26.1.166-173

Vasyl StefanykPrecarpathian National University

ФІЗИКА І ХІМІЯ ТВЕРДОГО ТІЛА
Т. 26, № 1 (2025) С. 166-173
Хімічні науки

UDK:546:548.736.4 882

ISSN 1729-4428 (Print)
ISSN 2309-8589 (Online)

Z. Shpyrka, Z. Staskevych, A. Horyn, V. Pavlyuk

Phase equilibrium diagram of the Y–Dy–Ge system at 870 K

Ivan Franko National University of Lviv, Lviv, Ukraine, z.shpyrka@gmail.com

The interaction of the components in the Y–Dy–Ge ternary system was investigated using the methods of X-ray phase analysis, microstructure and energy dispersive X-ray spectroscopy in the whole concentration range at temperature of 870 K. The existence of continuous solid solutions of substitution with the AlB_2 ($Y_{1-x}Dy_xGe_{1.5}$), Y_3Ge_5 ($Y_{3-x}Dy_xGe_5$), CrB ($Y_{1-x}Dy_xGe$), $Ho_{11}Ge_{10}$ ($Y_{11-x}Dy_xGe_{10}$), Sm_5Ge_4 ($Y_{5-x}Dy_xGe_4$) and Mn_5Si_3 ($Y_{5-x}Dy_xGe_3$) structure types was found.

Limited solid solutions of the substitution type, based on the binary compounds $YGe_{1,82}$ (0.20 at. part Dy), YGe_2 (~ 0,10 at. part Dy), $DyGe_{1,9}$ (0.07 at. part Y) and $DyGe_{1,85}$ (0.05 at. part Y) were observed.

The electrical and magnetic properties of the $Y_5Dy_{30}Ge_{65}$ ($DyGe_{1,85}$ structure type) and ($YGe_{1,82}$ structure type) alloys were studied. The phase $Y_{30}Dy_5Ge_{65}$ is Curie-Weiss paramagnet in the investigated temperature range. On the thermogram of the $Y_{10}Dy_{20}Ge_{65}$ alloy during cooling, we observe an intense peak at temperature of 1207.4 K (at maximum), the thermal effect of which reflects the formation of the $Dy_{1-x}Y_xGe_{1.85}$ phase.

Keywords: intermetallics, ternary system, phase equilibria, solid solution, physical properties.

Received 07 January 2025; Accepted 05 February 2025.

Introduction

The basis of many new materials are intermetallic compounds, which are formed during the chemical interaction of metals with each other, as well as with semi-metallic elements. Therefore, when studying the interaction of components in the corresponding systems, it is possible to obtain important information about the conditions of formation, temperature and concentration stability, microstructure, and crystal structure of the ternary phases, as a basis for the search for new materials. Phase diagrams for Ce–{Sc, Y, La, Gd, Lu}–Ge, Sc–{Nd, Y, Dy}–Ge [1], Sm–Dy–Ge [2] abd Tm–{Gd, Er}–Ge [3, 4] were constructed. Cross-sections for: $DyGe_2$–RGe_2 (R = Sm, Y, Gd, Tb, Ho, Er, Tm, Lu) [5], RGe_2–$LuGe_2$ (R = Sm, Pr, Nd, Gd, Dy) and $SmGe_2$–RGe_2 (R = Gd, Tb, Ho, Er, Tm) [6-10] were studied.

The purpose of this work is an experimental study of the interaction of components in the Y–Dy–Geternary system and the construction of a phase equilibrium diagram at 870 K and study of the physical properties.

I. Experimental

To construct a phase diagram of the Y–Dy–Ge system, the alloys were synthesized by the arc-melting of a charge of metals (the content of the basic component is not less than 99.7 wt.%) in an argon atmosphere (sponge titanium was used as a getter). For better homogenization, the samples were remelted twice. Homogenizing annealing of the alloys was carried out in vacuumed quartz ampoules at a temperature of 870 K for 720 hours with subsequent quenching in cold water.

The phase composition of the synthesized samples was determined based on the analysis of experimental powder diffraction patterns (DRON-4.0 diffractometer, Fe Kα radiation) by comparing them with theoretical diffraction patterns of pure components, binary compounds, and known ternary antimonides (PowderCell program [11]). Structural calculations were performed using WinCSD [12] program packages. The method of energy dispersive X-ray spectroscopy (EDRS) (raster microscope-microanalyzer REMMA 102–02, equipped with an X-ray analyzer with energy dispersive

spectroscopy) was used to control the chemical composition of the synthesized samples and determine the exact content of components in the phases. At least five measurements were performed for each phase in the sample.

Measurements of the temperature dependences of the electrical resistivity $\rho(T)$ and the thermopower coefficient $S(T)$ were carried out by the two-probe method in the range of 80–380 K on samples in the form of rectangular parallelepipeds measuring ~1.0×1.0×5 mm^3. Measurements of the thermopower coefficient $S(T)$ were performed by the potentiometric method in relation to copper. The dependence of the specific magnetic susceptibility $\chi(T)$ of the samples was determined by the relative Faraday method using a thermogravimetric device with an electronic microbalance EM–5–ZMP in a magnetic field H = 7.1 kOe.

The temperature limits of the stability of ternary compounds were investigated by the method of differential thermal analysis (DTA, synchronous thermal analyzer LINSEIS STA PT 1600). The samples were heated in an argon atmosphere up to 900 °C (1170 K) at a rate of 10 °C/min.

II. Results and discussion

To study the Y–Dy–Ge ternary system, information on phase diagrams of Y–Ge, Dy–Ge and Y–Dy binary systems was used from Refs. [13, 14]. At the temperature of the investigation, the formation of Y_5Ge_3 (Mn_5Si_3 structure type), Y_5Ge_4 (Sm_5Ge_4 structure type), $Y_{11}Ge_{10}$ ($Ho_{11}Ge_{10}$ structure type), YGe (CrB structure type), $YGe_{1,5}$ (AlB_2 structure type) and $YGe_{1,82}$ ($YGe_{1,82}$ structure type) compounds was confirmed in the Y–Ge system. The compound with α–$ThSi_2$ structure type exist with the composition $YGe_{1,7}$ [15]. Authors [16] indicate the composition Y_3Ge_5 (defective derivative of α–$ThSi_2$ structure type). Y_2Ge_7 phase not confirmed.

Seven intermetallic phases, Dy_5Ge_3 (Mn_5Si_3 structure type), Dy_5Ge_4 (Sm_5Ge_4 structure type), DyGe (CrB structure type), $DyGe_{1,59}$ (AlB_2 structure type), Dy_3Ge_5 (Y_3Ge_5 structure type), $DyGe_{1,85}$ ($DyGe_{1,85}$ structure type), $DyGe_3$ ($DyGe_3$ structure type) were found in the Dy–Ge system. The compounds $DyGe_{1,90}$ ($TbGe_2$ structure type), $Dy_{11}Ge_{10}$ ($Ho_{11}Ge_{10}$ structure type) and Dy_3Ge_4 (Er_3Ge_4 structure type), syntezied at 20 K is not observed on the phase diagram. The existence of the $DyGe_{1,90}$ and $Dy_{11}Ge_{10}$ compounds in the Dy–Ge system at a temperature of 870 K was confirmed by us during the study of the Sm–Dy–Ge system [2]. Under the conditions of our study, the existense of the Dy_3Ge_4 phase was not confirmed, the sample of the corresponding composition contained $DyGe_{1,59}$ and DyGe compounds in equilibrium. No binary compounds are formed in the system Y–Dy.

The phase equilibrium diagram of the Y–Dy–Ge system was constructed at 870 K based on the data from the X-ray phase, microstructural analyses, and scanning electron microscopy of the synthesized samples (Fig. 1). The binary compound $DyGe_{1,9}$ ($TbGe_2$ structure type) dissolves up to ~ 0.07 at. part Y. The lattice parameters: a = 0.40814(6), b = 2.9735(1), c = 0.3979(5) nm and V = 0.48301(1) nm^3 for $Y_3Dy_{31}Ge_{66}$; a = 0.40802(2), b = 2.97291(1), c = 0.39801(2) nm and V = 0.4828(1) nm^3 for $Y_7Dy_{27}Ge_{66}$ was calculated. The binary $YGe_{1,82}$ ($YGe_{1,82}$ structure type) and YGe_2 (α–$ThSi_2$ structure type) compounds dissolve 0.20 at. part and 0.10 at. part Dy respectively, at 870 K. Microstructural and EDX analyses were used to confirm the chemical and phase composition of the $Y_{22}Dy_{12}Ge_{66}$ and $Y_{25}Dy_9Ge_{66}$samples. Photographs of microstructures for some samples are shown in Figure 2.The composition dependencies of the cell parameters versus the Dy content in $Y_{1-x}Dy_xGe_{1,82}$ are shown in Figure 3 (*a*). Solubility of yttrium in binary compound $DyGe_{1,85}$ – 0.05 at. part.

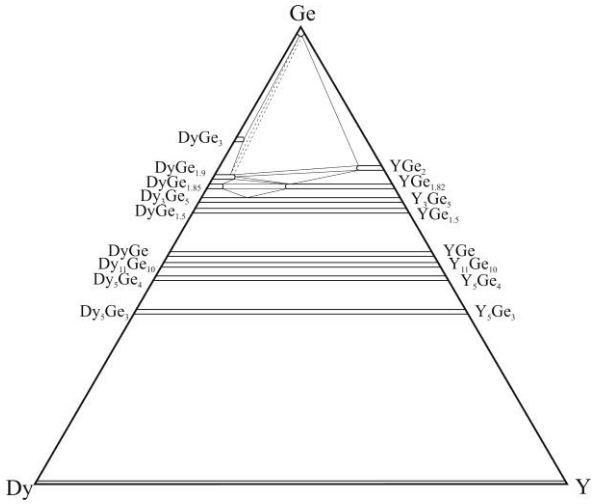

Fig. 1. Isothermal section of the Y–Dy–Ge system at 870 K.

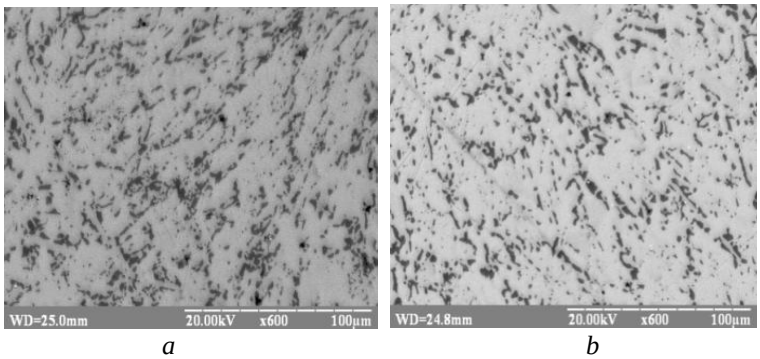

a *b*

Fig. 2. Microphotographs of the polished surface of the samples: *a* – $Dy_{12}Y_{22}Ge_{66}$ (gray phase –(Y, Dy)Ge_2; dark phase – Ge); *b* – $Dy_9Y_{25}Ge_{66}$ (gray phase –(Y, Dy)Ge_2; dark phase – Ge).

Six continuous solid solutions: $Y_{3-x}Dy_xGe_5$ (Y_3Ge_5 structure type), $Y_{1-x}Dy_xGe_{1.5}$ (AlB_2 structure type), $Y_{1-x}Dy_xGe$ (CrB structure type), $Y_{11-x}Dy_xGe_{10}$ ($Ho_{11}Ge_{10}$ structure type), $Y_{5-x}Dy_xGe_4$ (Sm_5Ge_4 structure type) and $Y_{5-x}Dy_xGe_3$ (Mn_5Si_3 structure type) are formed in the system. The cell parameters of the continuous solid solutions $Y_{3-x}Dy_xGe_5$, $Y_{1-x}Dy_xGe_{1.5}$, $Y_{1-x}Dy_xGe$, $Y_{11-x}Dy_xGe_{10}$, $Y_{5-x}Dy_xGe_4$ and $Y_{5-x}Dy_xGe_3$ were refined from X-ray powder diffraction data. The composition dependencies of the cell parameters versus the Dy content in $Y_{3-x}Dy_xGe_5$, $Y_{1-x}Dy_xGe_{1.5}$, $Y_{1-x}Dy_xGe$, $Y_{5-x}Dy_xGe_4$ and $Y_{5-x}Dy_xGe_3$ are shown in Figures 3–5, respectively.

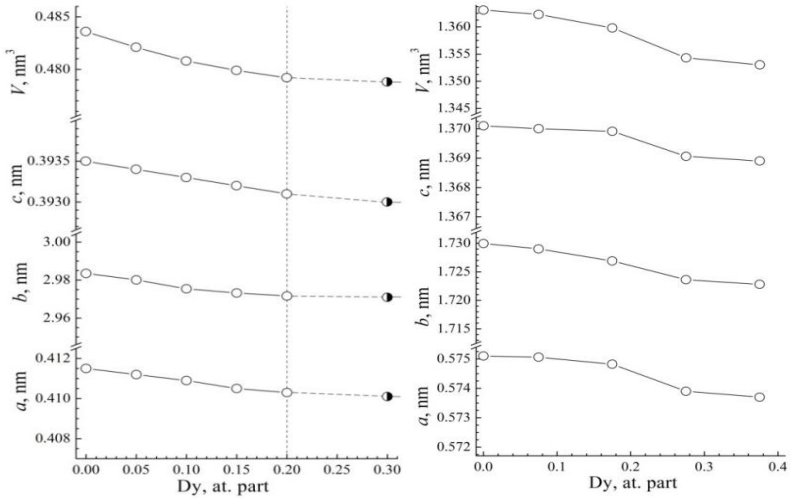

a *b*

Fig. 3. Cell parameters of the limited solid solution $Y_{1-x}Dy_xGe_{1,82}$ (a), of the continuous solid solutions $Y_{3-x}Dy_xGe_5$ (*b*).

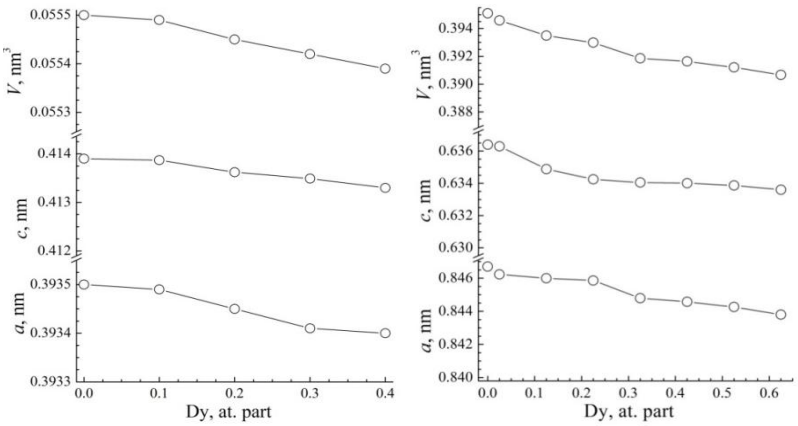

a *b*

Fig. 4. Cell parameters of the continuous solid solutions $Y_{1-x}Dy_xGe_{1,5}$ (*a*) and $Y_{5-x}Dy_xGe_3$ (*b*).

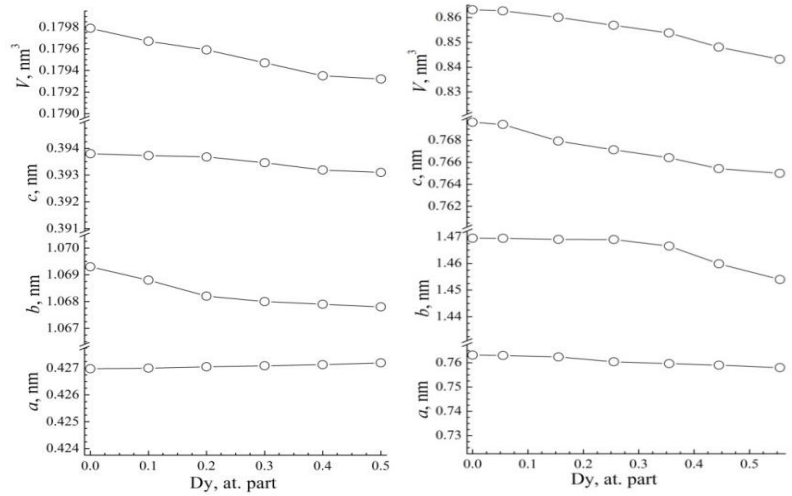

a *b*

Fig. 5. Cell parameters of the continuous solid solutions $Y_{1-x}Dy_xGe$ (*a*) and $Y_{5-x}Dy_xGe_4$ (*b*).

III. Physical properties of the alloys

Alloys from the regions of solid solutions $Y_{1-x}Dy_xGe_{2-y}$ and $Y_{1-x}Dy_xGe_{1,5}$ were chosen for the study of physical properties. Temperature dependences of electrical resistivity $\rho(T)$ and differential thermopower $S(T)$ were investigated for samples $Y_{30}Dy_5Ge_{65}$ and $Y_5Dy_{30}Ge_{65}$ in the temperature range 80–380 K (Fig. 6). The gradual increase in electrical resistivity with increasing temperature and its small values prove that these phases are characterized by a metallic type of conductivity in the investigated temperature range. The linear character of the temperature dependences of $\rho(T)$ in the temperature range of 80–380 K indicates the predominant phonon mechanism caused by the scattering of electrons by the thermal vibrations of the atoms of the crystal lattice. The significant increase in resistivity above 350 K is possibly caused by the enhancement of phonon scattering. The dependences of the differential thermopower from the temperature for $Y_{30}Dy_5Ge_{65}$ (*a*) and $Y_5Dy_{30}Ge_{65}$ (*b*) samples are shown in Fig. 7. A small positive value of the differential thermopower confirms the belonging of these samples to materials with metallic conductivity. On the $S(T)$ dependences, there is a noticeable increase in the differential thermopower for both samples with an increase in temperature. At the same time, for the $Y_5Dy_{30}Ge_{65}$ sample, its value is higher compared to $Y_{30}Dy_5Ge_{65}$, which can be explained by the greater contribution of dysprosium atoms to the value of the thermopower coefficient.

Dependencies of electrical resistivity on temperature for $Y_{30}Dy_{10}Ge_{60}$, $Y_{20}Dy_{20}Ge_{60}$ and $Y_{10}Dy_{30}Ge_{60}$ samples are shown in Fig. 8. The samples are characterized by small values of electrical resistivity (Table 1), the gradual increase of which with temperature indicates a metallic type of conductivity. The linear nature of the temperature dependences $\rho(T)$ within T = 80–350 K confirms that the main contribution to the electrical resistance gives phonon electron scattering, which is enhanced above 350 K.

The results of measurements of the temperature dependencies of the differential thermopower coefficient for samples $Y_{30}Dy_{10}Ge_{60}$, $Y_{20}Dy_{20}Ge_{60}$ and $Y_{10}Dy_{30}Ge_{60}$ (Fig. 9) show small negative values, which are characteristic of compounds with a metallic type of conductivity. With an increase in the Dy content at higher temperatures, there is a tendency to shift the course of the dependencies towards positive values of the thermopower coefficient.

The temperature dependence of the magnetic susceptibility $\chi(T)$ was investigated for the $Y_{30}Dy_5Ge_{65}$ sample (Fig. 10, *a*) in the magnetic field H = 7.1 kOe, it changes hyperbolically and corresponds to the Curie-Weiss law. From the inverse dependence of $\chi^{-1}(T)$ (Fig. 10, *b*), the paramagnetic Curie temperature (Θ_p= 45.35 K) was determined, and the effective magnetic moment per rare earth metal atom $\mu_{eff.}$ = 10.83 μ_B was obtained, close to the theoretically calculated for the Dy^{3+} ion ($\mu_{theor.}$ = 10.65 μ_B). The analysis of the results of the magnetic susceptibility measurements indicate that the $Y_{30}Dy_5Ge_{65}$ sample is a Curie-Weiss paramagnet, in which the Dy atoms are in the Dy^{3+} state. In contrast, the Y and Ge atoms are non-magnetic.

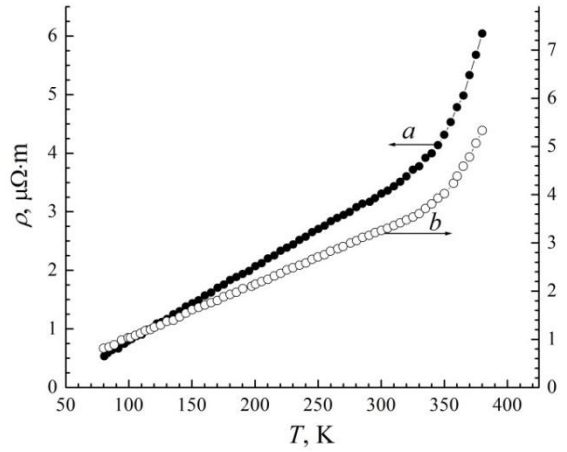

Fig. 6. The temperature dependence of electrical resistivity of $Y_{30}Dy_5Ge_{65}$ (*a*) and $Y_5Dy_{30}Ge_{65}$ (*b*).

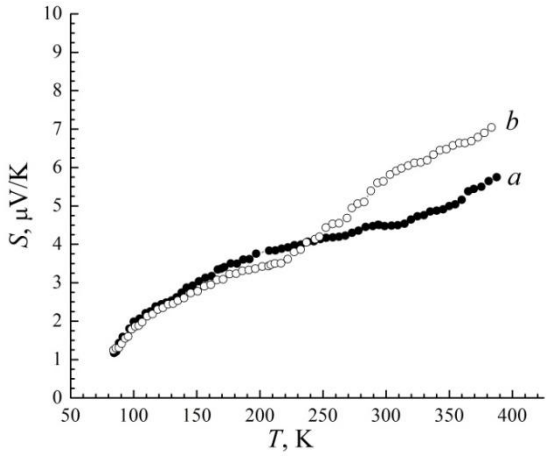

Fig. 7. Temperature dependencies of thermopower of $Y_{30}Dy_5Ge_{65}$ (*a*) and $Y_5Dy_{30}Ge_{65}$ (*b*).

Table 1.

Electrontransport characteristics of samples

Sample	ρ, μΩ·m			S, μV/K		
	80 K	273 K	380 K	80 K	273 K	380 K
$Y_{30}Dy_5Ge_{65}$	0.541	3.000	6.015	1.089	4.166	5.637
$Y_5Dy_{30}Ge_{65}$	0.812	2.967	5.339	1.199	4.958	6.959
$Y_{30}Dy_{10}Ge_{60}$	0.405	1.058	2.905	0.718	1.469	2.439
$Y_{20}Dy_{20}Ge_{60}$	0.424	0.839	1.206	1.567	1.666	1.294
$Y_{10}Dy_{30}Ge_{60}$	0.683	1.796	3.458	1.421	0.923	0.140

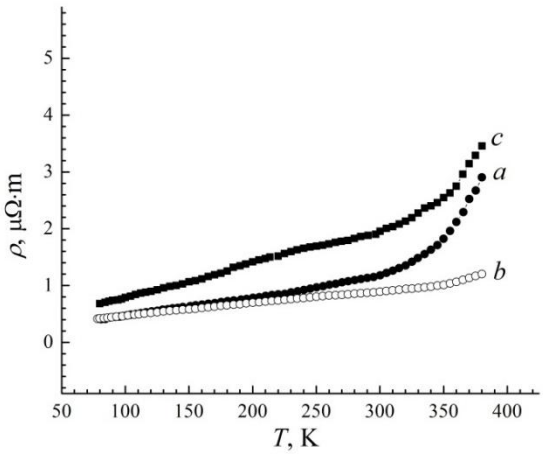

Fig. 8. Temperature dependencies of the electrical resistivity of $Y_{30}Dy_{10}Ge_{60}$ (*a*), $Y_{20}Dy_{20}Ge_{60}$ (*b*) and $Y_{10}Dy_{30}Ge_{60}$ (*c*).

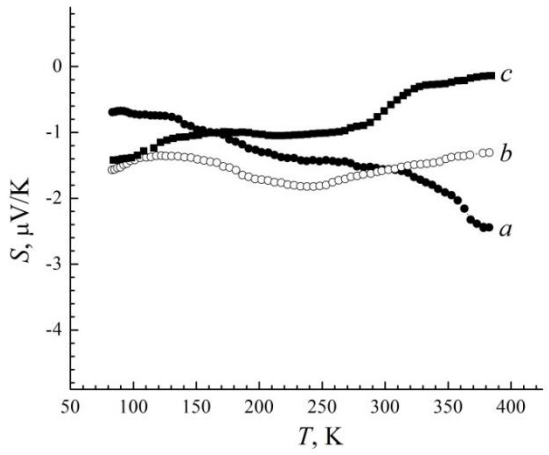

Fig. 9. Temperature dependence of the differential thermopower of $Y_{30}Dy_{10}Ge_{60}$ (*a*), $Y_{20}Dy_{20}Ge_{60}$ (*b*) and $Y_{10}Dy_{30}Ge_{60}$ (*c*).

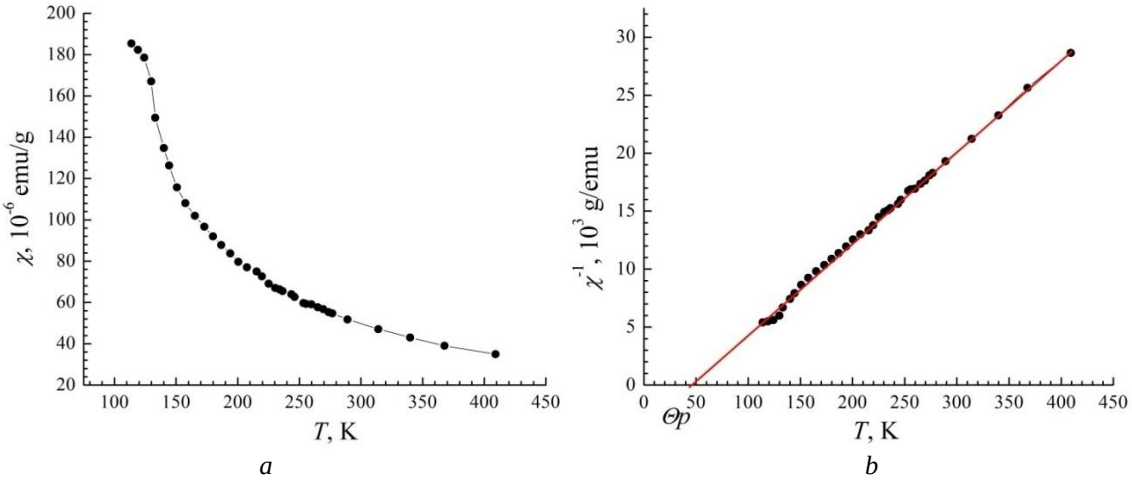

a *b*

Fig. 10. Temperature dependence of the magnetic susceptibility (a) and of the inverse magnetic susceptibility (*b*) of $Y_{30}Dy_5Ge_{65}$sample.

For the $Y_{15}Dy_{20}Ge_{65}$ sample, a study using differential scanning calorimetry was performed (Fig. 11). Two peaks were detected on the heating curve and the cooling curve. When cooling the alloy, an intense peak is observed at 1207.4 K (at the maximum), the thermal effect of which reflects the formation of the $Y_{1-x}Dy_xGe_{1,85}$ phase according to the transformation:

$$L+\beta\text{-}Dy_{1-x}Y_xGe_{1.61} \rightarrow Y_{1-x}Dy_xGe_{1.85} \text{ at } 1207.4 \text{ K } (\sim 0.65 \text{ at. part Ge}).$$

At a lower temperature of 1147.4 K (at the maximum), a peak of lower intensity is observed, which corresponds to the transformation:

$$L + Dy_{1-x}Y_xGe_{1.85} \rightarrow Dy_{1-x}Y_xGe_3 \text{ at } 1147.4 \text{ K } (\sim 0.75 \text{ at. part Ge}).$$

It should be noted that the formation temperature of the $Dy_{1-x}Y_xGe_{1.85}$ solid solution (1207.4 K) has an intermediate value compared to the temperatures of formation of the binary phases: 1240 K for $DyGe_{1.85}$ and 1183 K for $YGe_{1.82}$.

$Y_{1-x}Dy_xGe_{2-y}$ and $Y_{1-x}Dy_xGe_{1,5}$ solid solutions contain a significant content of Ge as a semiconducting element and a sufficiently high concentration of Y and Dy as doping components, which determines the metallic type of conductivity of the samples, as a result of which the electrical resistivity enlarges linearly with increasing temperature. The magnitude of the electrical resistivity of the investigated phases is of the same order as the values of the electrical resistivity of the pure components yttrium (ρ_{293}(Y) = 0.65 μΩ·m) and dysprosium (ρ_{273}(Dy) = 0.90 μΩ·m), which indicates their determining role in conductivity of these solid solutions.

For these two series of samples, a different effect of *R* substitution on their electrical resistivity is observed.

For the $Dy_{1-x}Y_xGe_{2-y}$ series of samples with increasing Y

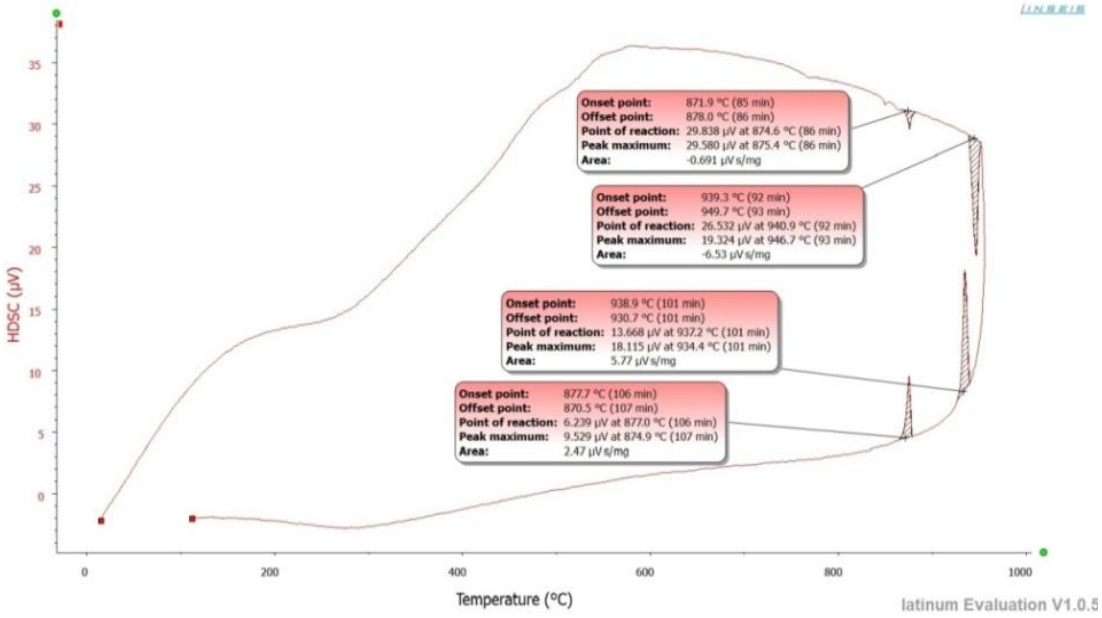

Fig. 11. DSC curveforthe $Y_{15}Dy_{20}Ge_{65}$ sample.

Table 2.

Magnetic characteristics of compounds and sample

Compound (sample)	Structuretype	T_N	$\mu_{e\phi}$	μ_{Teop}	θ_p	Ref.
$HoGe_{1,85}$	$DyGe_{1,85}$	12K	-	10.61	-	[18]
$ErGe_{1,83}$	$DyGe_{1,85}$	6K	10.3	9.58	8K	[19]
$Y_{30}Dy_5Ge_{65}$	$YGe_{1,82}$	-	10.83	10.65	45.4K	[20]

content at higher temperatures, the electrical resistivity reaches higher values, possibly due to the greater ability of yttrium to thermal fluctuations as a lighter element compared to dysprosium. For a series of samples $Dy_{1-y}Y_yGe_{1,5}$, on the contrary, an increase in the Dy content leads to higher values of electrical resistivity, which may be associated with a greater scattering of electrons on the magnetic atoms of Dy.

In Ref. [17], low-temperature electrical resistivity studies were carried out for YGe_2 and $LaGe_2$ compounds using the four-probe method, and transitions to the superconducting state were established at temperatures of 3.8 and 2.65 K, respectively. The temperature range of 80–380 K used in our study did not allow us to obtain the presence of atransition to superconductivity.

Even though the values of thermopower coefficient for Dy (-2.2 µV/K) and Ge (+3.6 µV/K) have opposite signs, for both series of studied samples, the effect of dysprosium is observed, the increase in the content of which in the samples leads to an increase in positive values of thermopower coefficient.

An interesting fact is obtaining values of thermopower opposite signs for samples $Y_{1-x}Dy_xGe_{1,82}$ and $Y_{1-x}Dy_xGe$ with a slight difference in the concentration of Ge, which is obviously due to the effect of Ge, as an element with a higher positive value of thermopower coefficient (α_{273}(Ge) = +3.6 µV/K) compared to Y (α_{273}(Y) = -0.6 µV/K) and Dy (α_{273}(Dy) = -2.2 µV/K).

Magnetic ordering was not observed in the studied temperature range for the $Y_{30}Dy_5Ge_{65}$ sample due to the limitation of the temperature range of the device measurements. The analysis of literature data showed for compounds with a high germanium content $HoGe_{1,85}$ and $ErGe_{1,83}$, the presence of antiferromagnetic ordering at T_N = 12 K and T_N = 6 K, respectively, which can be expected from our samples at helium temperatures.

Similar to the compound $ErGe_{1.83}$ with an effective magnetic moment $\mu_{eff.}$ = 10.3 μ_B, the $Y_{30}Dy_5Ge_{65}$ sample also exhibits a slightly higher magnetic moment and paramagnetic Curie temperature (table 2).

The investigation of the Y–Dy–Ge ternary system, literature data about the R–R′–Ge (R and R' two different rare earth) ternary systems confirms that continuous solid solution are formed when binary germanides crystallized in the same structure types. When binary germanides crystallized in the different structure types, we see formation of the ternary compounds and limited solid solutions and the length of these solid solution is determined by the sizes of the substituted atoms.

Conclusions

The phase equilibrium diagram of the Y–Dy–Ge ternary system was constructed at a temperature of 870 K in the whole concentration range based on the results of an experimental study of the interaction of components. The investigated system at 870 K is characterized by the formation of six continuous solid solution and limited solid solutions. The investigated of the electrical properties of the alloys indicates of the metallic type of conductivity in the temperature range 80–380 K. The $Y_{30}Dy_5Ge_{65}$ phase is Curie-Weiss paramagnet in the investigated temperature range.

Acknowledgement

The authors Z. Shpyrka, A. Horynand V. Pavlyuk are greatly thankful to the Simons Foundation (Award ID: 1290588) for financial support.

Shpyrka Zinoviya *– Ph.D., Associate Professor, Associate Professor of the Department of Inorganic Chemistry, Ivan Franko National University of Lviv*;
Staskevych Zoriyana **–** student of Chemical faculty, Ivan Franko National University of Lviv;
Horyn Andriy – Ph.D., Senior Scientist of Ivan Franko National University of Lviv;
Pavlyuk Volodymyr – D.Sc., Professor, Professorof the Depertament of Inorganic Chemistry, Ivan Franko National University of Lviv.

[1] O. I. Bodak, Z. M. Shpyrka, I. R. Mokra, *Peculiarities of the interaction of the components in the systems of two rare earth metals and germanium*, J. Alloys Comp., 247, 217 (1997); https://doi.org/10.1016/S0925-8388(96)02589-3.
[2] Z. Shpyrka, K. Kluziak, B. Rożdżyńska-Kiełbik, A. Stetskiv, V. Pavlyuk, *The isothermal section of the phase diagram of Sm–Dy–Ge ternary system at 873 K*, J. Phase Equilib. Diff., 39(6), 750(2018); https://doi.org/10.1007/s11669-018-0665-9.
[3] T. Melnyk, Z. Shpyrka, *The investigation of the solid Gd–Tm–Ge system at 870 K*, Visnyk Lviv Univ. Ser. Chem., 52, 3 (2011).
[4] N. Guk, Z. Shpyrka, P. Starodub, *The investigation of the Er–Tm–Ge system in the 0,5–1,0 at. part. of Ge region*,Visnyk Lviv Univ. Ser. Chem., 50, 18 (2009).
[5] Z. Shpyrka, L. Drab, *The investigation of the solid solutions $DyGe_2$–RGe_2, R – Y, Gd, Tb, Ho, Er, Tm and Lu at 600 °C*, Visnyk Lviv Univ. Ser. Chem., 49, 98 (2008).
[6] Z. Shpyrka, Yu. Cheh, O. Yuziv, N. German, V. Pavlyuk, *X-ray investigation of alloys on the cross sections RGe_2–$LuGe_2$ (R – Pr, Nd) and $SmGe_2$–$R'Ge_2$ (R' – Gd, Tb, Ho, Er, Tm)*, Visnyk Lviv Univ. Ser. Chem., 60, 64 (2019); http://dx.doi.org/10.30970/vch.6001.064.
[7] Z. Shpyrka, N. German, *Phase equlibria in the quasibinary sections $GdGe_2$–RGe_2 (R = Ho, Lu)*, Coll. Abst. XVIII Int. Sem. Phys. and Chem. of Solids, 54 (2012).
[8] Z. Shpyrka, N. German, V Pavlyuk, *The investigation of the $GdGe_2$–$LuGe_2$ system at 870 K*, Visnyk Lviv Univ, Ser. Khim., 55(1), 37 (2014).
[9] V. Vorotnyak, Z. Shpyrka, N. German, *The quasibinary sections $GdGe_2$–$HoGe_2$ at 870 K*, Visnyk Lviv Univ. Ser. Chem., 54, 45 (2013).
[10] O. Kravchuk, Z.Shpyrka, N. German, V. Pavlyuk, *The investigation of the quazibinary cross section $SmGe_2$–$LuGe_2$*, Visnyk Lviv Univ. Ser. Chem., 59, 83 (2018); https://doi.org/10.30970/vch.5901.083.
[11] W. Kraus, G. Nolze, *POWDER CELL – a program for the representation and manipulation of crystal structures and calculation of the resulting X-ray powder patterns*, J. Appl. Crystallogr., 29, 301 (1996); https://doi.org/10.1107/S0021889895014920.
[12] L. Akselrud, Yu. Grin, *WinCSD: Soft ware package for crystallographical calculations (Version 4)*, J. Appl. Crystallogr., 47, 803 (2014); https://doi.org/10.1107/S1600576714001058.
[13] T. B. Massalski, *Binary Alloy Phase Diagrams*, ASM, MetalsPark, Ohio(1990).
[14] H. Okamoto, *Desk Handbook: Phase Diagrams for Binary Alloys*, Materials Park (OH): ASM (2000).
[15] O. Schob, E. Parthe, *Digermanide des Scandium and Yttrium*, Monatsheftefuerchemie, 95, 1466 (1964).
[16] V. A. Bruskov, O. I. Bodak, E. I. Gladyshevskii, *The Crystal Structure of Y_3Ge_5 ($YGe_{1,7}$)*, J. Phys. Cryst., 28(2), 151 (1983).
[17] A. K. Ghosh, D. H. Douglass, *Superconductity in non-cubic crystal structures*, Solid St. Commun., 23, 223 (1997); https://doi.org/10.1016/0038-1098(77)90447-1.
[18] O. Zaharko, P. Schobinger Papamantellos, C. Ritter, *Antiferromagnetic ordering in the novel Ho_3Ge_5 and $HoGe_{1,85}$ compounds studied by X-ray and neutron diffraction*, J. Alloys Comp., 280, 4 (1998); https://doi.org/10.1016/S0925-8388(98)00555-6.
[19] O. Oleksyn, P. Schobinger Papamantellos, C. Ritter, C. *H. de Groot, K. H. J. Buschow*,Structure and magnetic ordering in the defect compound $ErGe_{1,83}$, J. Alloys Comp., 252, 53 (1997).
[20] Z. S. Staskevych, A. M. Goryn, Z. M. Shpyrka, *The investigation of the physical properties of alloys of the ternary Y–Dy–Ge system*, Coll. Abst. X Ukr. Sci. conf. Students and graduate students "Chemical Karazinreadings – 2018". 53 (2018).

З. Шпирка, З. Стаськевич, А. Горинь, В. Павлюк

Діаграма фазових рівноваг системи Y–Dy–Ge при 870 K

Львівський національний університет імені Івана Франка, Львів, Україна, z.shpyrka@gmail.com

Взаємодія компонентів у потрійній системі Y–Dy–Ge досліджена в повному концентраційному інтервалі за температури 870 K методами рентгенівського і мікроструктурного аналізів, енергодисперсійної рентгенівської спектроскопії. Між ізоструктурними бінарними германідами ітрію та диспрозію утворюються неперервні тверді розчини заміщення $Y_{1-x}Dy_xGe_{1,5}$ (структурний тип AlB_2), $Y_{3-x}Dy_xGe_5$ (структурний тип Y_3Ge_5), $Y_{1-x}Dy_xGe$ (структурний тип CrB), $Y_{11-x}Dy_xGe_{10}$ (структурний тип $Ho_{11}Ge_{10}$), $Y_{5-x}Dy_xGe_4$ (структурний тип Sm_5Ge_4) та $Y_{5-x}Dy_xGe_3$ (структурний тип Mn_5Ge_3). Сполуки $YGe_{1,82}$ (структурний тип $YGe_{1,82}$) та YGe_2 (структурний тип α-$ThSi_2$) розчиняють 0,20 та ~ 0,10 ат. частки Dy відповідно, $DyGe_{1,9}$ (структурний тип $TbGe_2$) ~ 0,07 ат. частки Y, $DyGe_{1,85}$ (структурний тип $DyGe_{1,85}$) – 0,05 ат. частки Y.

Досліджено електричні та магнітні властивості сплавів складу $Y_5Dy_{30}Ge_{65}$ (структурний тип $DyGe_{1,85}$) та $Y_{30}Dy_5Ge_{65}$ (структурний тип $YGe_{1,82}$). Зразок складу $Y_{30}Dy_5Ge_{65}$ є парамагнетиком Кюрі-Вейса. На термограмі при охолодженні сплаву $Y_{10}Dy_{20}Ge_{65}$ спостерігаємо інтенсивний пік за температури 1207,4 K (у максимумі), термічний ефект якого відображає утворення фази $Y_{1-x}Dy_xGe_{1,85}$.

Ключові слова: інтерметаліди, потрійна система, фазові рівноваги, твердий розчин, фізичні властивості.